



Imaging of Structural Plasticity of Dendritic Spines with Two-Photon Microscopy

Takeo Saneyoshi  and Yasunori Hayashi 

Abstract

Plasticity of synaptic transmission underlies learning and memory. It is accompanied by changes in the density and size of synapses, collectively called structural plasticity. Therefore, understanding the mechanism of structural plasticity is critical for understanding the mechanism of synaptic plasticity. In this chapter, we describe the procedures and equipment required to image structural plasticity of a single dendritic spine, which hosts excitatory synapses in the central nervous system, and underlying molecular interactions/biochemical reactions using two-photon fluorescence lifetime microscopy (2P-FLIM) in combination with Förster resonance energy transfer (FRET)-based biosensors.

Key words Two-photon fluorescence lifetime measurement microscopy, Dendritic spine, Synapse, Actin cytoskeleton, LTP, CaMKII

1 Introduction

In the neuronal network, synapses formed between neurons mediate information transmission. Synapses are functionally and structurally plastic to support higher order brain functions such as learning and memory. In representative forms of synaptic plasticity, long-term potentiation (LTP) and long-term depression (LTD), changes in spine density and size have been observed [1–5]. During the induction of Long-term potentiation (LTP), Ca^{2+} influx through N-methyl-D-aspartate (NMDA)-type glutamate receptors and the resulting activation of Ca^{2+} /calmodulin-dependent protein kinase II (CaMKII) triggers activation of signal transduction that eventually leads to the regulation of actin cytoskeleton [6, 7] and enlarges dendritic spines, a process called structural LTP (sLTP). This may act to translocate α -amino-3-hydroxy-5-methyl-4-isoxazolepropionate (AMPA)-type glutamate receptors to the enlarged synaptic surface and to maintain synaptic strength by providing new binding sites for synaptic molecules [6, 8–12].

Therefore, visualization of structural changes and underlying regulatory pathways during synaptic plasticity is crucial for understanding the mechanisms of learning and memory.

Traditionally, the biochemical signaling of these processes has been studied using homogenates of cells. However, this approach has major drawbacks in studying spatiotemporal dynamics. In this regard, the introduction of several key technologies has significantly advanced the field. First, the uncaging of caged-glutamate using a two-photon laser allows us to reliably induce LTP or LTD in a single spine under observation of a living neuron [13, 14]. Second, Förster resonance energy transfer (FRET), a non-radiative transfer of energy from an excited donor fluorophore to an acceptor fluorophore, can be used to monitor an interaction or a conformational change of proteins fused to different fluorophores [1, 15, 16]. It can be used as a molecular ruler to monitor the biochemical signaling that occurs within single dendritic spines under observation [17]. Finally, fluorescence lifetime imaging microscopy (FLIM), a microscopic method that detects the decay of fluorescence emission after excitation, is used to detect FRET. It has several advantages over conventional ratio-metric imaging. In particular, FLIM only uses the signal from the donor, and is therefore not affected by volume changes or the localization of proteins. This is particularly advantageous in spines where molecules are dynamically moving [18].

In this chapter, we describe the protocols for imaging structural plasticity of a dendritic spine, including sLTP induction and FLIM-FRET measurements using rat hippocampal slice cultures under two-photon laser scanning microscopy [19]. We use the TIAM1—CaMKII interaction as an example [19]. We will not discuss the design of FLIM-FRET probes; readers can refer to other reviews for further information [16].

2 Materials

2.1 Hippocampal Slice Cultures

1. Hippocampal culture media: 80% minimum essential medium (MEM) (Hanks' salts with L-glutamine, Gibco, 11575-032), 20% horse serum (Biowest, S0910), supplemented with 30 mM HEPES, 26.6 mM D-glucose, 5.8 mM NaHCO₃, 1 mM CaCl₂, 5 mM MgSO₄, 0.5 µg/mL insulin (Nacalai Tesque, 19251-24), 0.0012% ascorbic acid, pH 7.4, osmolality 320 ± 10 mOsm/L (Wescor 5600, vapor pressure osmometer, Elitech Group Inc.).
2. Dissection solution (2.5 mM KCl, 26 mM NaHCO₃, 1 mM NaH₂PO₄, 11 mM glucose, 238 mM sucrose, 1 mM CaCl₂, and 5 mM MgCl₂). Bubble with mixed gas containing 95% O₂ and 5% CO₂ for 20–30 min.

3. Artificial cerebrospinal fluid (ACSF): 119 mM NaCl, 2.5 mM KCl, 26.2 mM NaHCO₃, 1 mM NaH₂PO₄, 11 mM glucose, 4 mM CaCl₂, 1 μM tetrodotoxin (TTX), and 50 μM picrotoxin. Bubble with mixed gas containing 95% O₂ and 5% CO₂ for 20–30 min. Osmolality should be in the range of 320 ± 10 mOsm/L.
4. Uncaging ACSF: ACSF contains 2.5 mM 4-methoxy-7-nitroindolil (MNI)-L-glutamate (caged-glutamate. Tocris, No. 1490).

2.2 Bullet for Gene-Gun

1. DNA constructs are in a pCAGGS vector [20]. Since original enhanced green fluorescent protein (EGFP) tends to form dimers, we routinely use monomeric GFP with a A206K mutation, especially for fusion proteins.
2. 100% ethanol (desiccated with molecular sieves).
3. 0.05 M spermidine (Sigma, S-0266).
4. 1.0 M CaCl₂.
5. 20 mg/mL polyvinylpyrrolidone (Sigma, PVP360).
6. Gold powder (0.3–3 μm, Chempur, 009150-5).
7. Helios[®] Gene Gun system (Bio-Rad).
8. Helium tank.

2.3 Two-Photon Microscopy Setting

1. Two-photon microscope (FV1000ME, Olympus), 10× and 60× water immersion objective lens.
2. Two Ti-sapphire tunable pulsed lasers (Mai-tai DeepSee, Spectra-Physics), set at 910 nm for imaging, 720 nm for uncaging.
3. Fluorescent beads (0.5 μm diameter, Fluoresbrite YG, Polyscience, Inc.) covalently linked onto collagen-coated glass bottom dish.
4. Imaging chamber for circulation of ACSF with caged-glutamate (Fig. 1).

2.4 Fluorescent Lifetime Imaging Microscopy

1. A separate FLIM PC with time-correlated single photon counting (TCSPC) board (SPC-150, Becker-Hickl) and data acquisition software (Becker-Hickl).
2. A part of the excitation laser light is reflected on the surface of a cover glass placed in the light path and introduced into a photodiode module (PHD-400 PIN, Becker and Hickl). Then the pulsing is fed into the TCSPC board for synchronizing photon counting with excitation.
3. The PC controlling the two-photon microscope sends the frame start and sweep start timing signal to the FLIM PC.

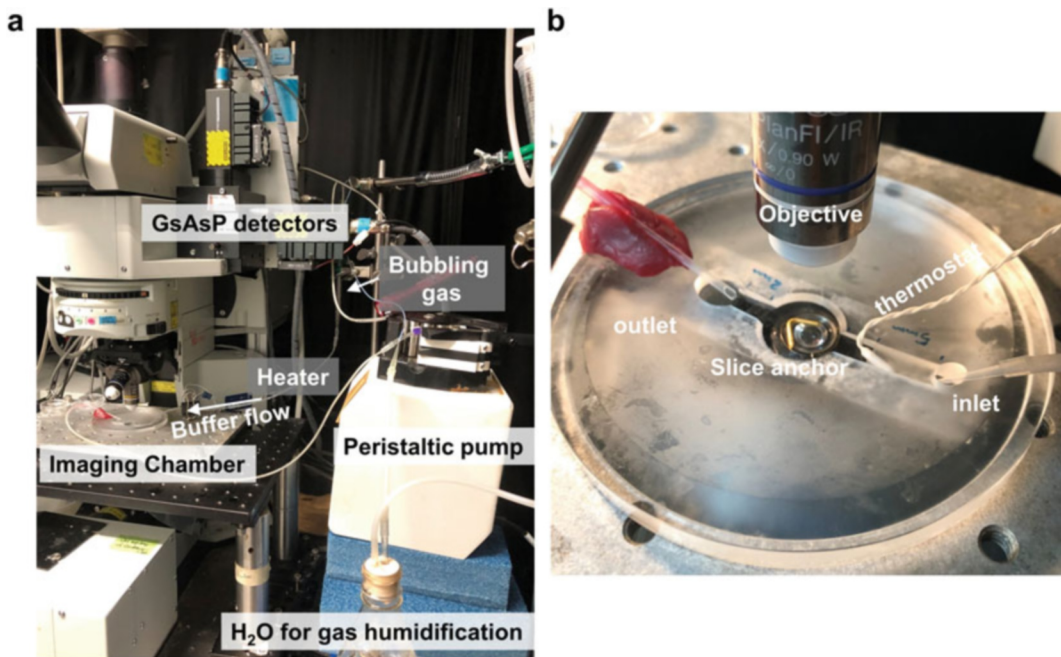


Fig. 1 Two-photon microscope with FLIM capability. **(a)** A FLIM detector is outfitted to a commercially available two-photon microscope (Olympus). ACSF is circulated through a peristaltic pump. The mixed gas is humidified with distilled water before bubbling the ACSF. **(b)** Imaging chamber. The slice is placed in the center of the chamber and held in place by the slice anchor. The temperature of the ACSF is controlled by the temperature controller via a thermostat

4. Gallium arsenide phosphide (GaAsP) detector (H7422-40, Hamamatsu Photonics) with custom-made power supply and amplifier (Olympus).

2.5 Image Analysis

FIJI (ImageJ) analysis for volume of dendritic spines.
 Custom-made program to analyze FLIM images.

3 Methods

3.1 Hippocampal Slice Culture

It is generally perceived that synaptic plasticity is difficult to induce in dissociated culture. Therefore, we use hippocampal organotypic slice culture. Hippocampal slice cultures are prepared from postnatal day 6–9 rat pups of both sexes [19, 21]. The hippocampi are dissected out in ice-cold dissection solution. Slices (350 μm thick) are prepared using a McIlwain Tissue Chopper (TC752, Cavey Laboratory Engineering Co. Ltd.) and plated on a cell culture insert (Millicell CM, Millipore, PICM0RG50) in a six-well plate containing 1 mL of culture medium. After removing the excess dissection solution around the slice, the hippocampal slice cultures are placed in a CO_2 incubator (35 $^\circ\text{C}$, 5% CO_2 , 95% air) and the culture medium is changed every 2–3 days.

3.2 Gene-Gun Bullet Preparation and Gene Transfer into Slices

Prepare gene-gun bullets using 12.5 mg of gold powder and 50 μg of plasmid DNA according to the manufacturer's instructions (Bio-Rad). Bullets are stored in a plastic scintillation vial together with a desiccator (e.g., silica gel or Drierite) at $-25\text{ }^{\circ}\text{C}$. Plasmids are transfected at 5–7 DIV using the gene-gun at a gas pressure of 180–200 psi. Expression of exogenous fluorescent proteins is imaged 2–7 days after the transfection.

To analyze the structural changes of the spine during LTP, GFP or another fluorescent protein can be used as a volume filler. For molecular dynamics analysis in a spine during LTP, GFP-fusion protein and DsRed2 as volume filler are co-expressed from a single gene-gun bullet. For gene knockdown experiments with shRNA, a knockdown vector construct such as pSuper and volume filler can be co-expressed as a transfection marker. The ratio of plasmid DNAs should be determined empirically.

3.3 Two-Photon Imaging and the Glutamate Uncaging Stimulation

1. For two-photon imaging and stimulation, one laser is tuned at 910 nm to image GFP, and the other laser at 720 nm to uncage the caged-glutamate. Before starting the experiment, the two lasers are adjusted using fluorescent beads (0.5 μm diameter). The images of fluorescent beads from the imaging laser and the stimulating laser must be perfectly overlapped within an error of $<50\text{ nm}$ at the center of the field of view. The power of the stimulation laser is adjusted at 5 mW under the 60 \times objective using the power meter (LaserCheck, Coherent, Inc.).
2. Prepare perfusion. To perfuse ACSF, we use a peristaltic pump (MINIPULS 3, Gilson), and aerate the ACSF with a mixed gas (95% O_2 , 5% CO_2), pre-humidified by passing distilled water through once. Turn on the temperature controller (TC324B, Warner Instruments) set to $30\text{ }^{\circ}\text{C}$. We typically use 6 mL of ACSF for circulation to save the caged glutamate.
3. Select an appropriate slice containing healthy GFP-positive neurons in area CA1, cut the membrane containing the slice from the culture-insert ($\sim 5 \times 5\text{ mm}$), and place it in the chamber. Immobilize it with a slice anchor (Warner Instruments) or platinum wire (Fig. 1).
4. Search for neurons expressing fluorescent proteins under illumination with a mercury lamp and an appropriate filter set through a 10 \times objective. Then use a 60 \times objective to find an isolated dendritic spine. Add the caged-glutamate to the ACSF to a final concentration of 2.5 mM. Incubate the slice for 30–40 min to stabilize the slice.
5. Find a spine separated from the dendritic shaft. The spines are imaged through a 60 \times objective and digitally zoomed at 10 \times . Using a Z-series of 512×512 -pixel X-Y scans taken every 0.5–1 μm in depth, acquire images for 15 min as a baseline,

every 5 min, and then 35 min after the uncaging stimulation. The GFP signal is imaged through a 495–540 nm band-pass filter, and the red fluorescent protein (RFP) signal through a 575–630 nm band-pass filter with a 510 nm short-pass or long-pass dichroic mirror.

6. Stimulate a single spine by uncaging the caged-glutamate. The uncaging laser pulse should be given $\sim 0.5 \mu\text{m}$ away from the tip of the dendritic spine at 2 msec for 30 pulses at 1 Hz or 4 msec for 30 pulses at 0.5 Hz [19, 22].
7. When an LTP measurement is completed, if there are multiple neurons expressing fluorescent protein, we select another neuron and repeat the recording of two or three neurons from one slice. When changing to another slice, we measure the osmolality and adjust it to $320 \pm 10 \text{ mOsm/L}$ with distilled water.
8. For image analysis, we subtract the background from each image. The change in spine volume is expressed as the difference of the averaged intensities from the baseline. Synaptic trafficking of protein can be calculated as the ratio between fluorescence of a protein of interest and volume filler [22].

3.4 2P-FLIM During Structural LTP

1. We typically use monomeric GFP as a donor and mCherry as an acceptor. For the TIAM1-CaMKII interaction, we used TIAM1 tagged with GFP at the carboxy tail and CaMKII tagged with mCherry at both ends (Fig. 2). The fluorescence lifetime is measured using the TCSPC system as described above at 910 nm excitation.
2. GFP emission light is filtered through a $510 \pm 35 \text{ nm}$ band-pass filter and a 680 nm short-pass blocking filter (Omega Optical). Images are binned at 64×64 pixels to increase the number of photons per pixel for accurate lifetime calculations.

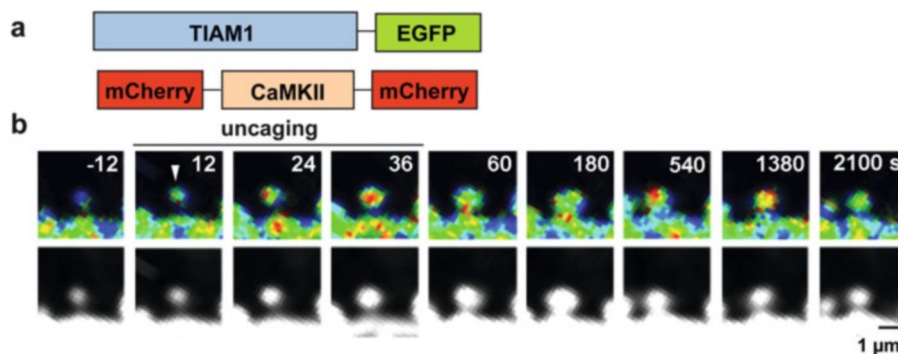


Fig. 2 FLIM-FRET imaging. (a) FLIM-FRET probe used to detect the interaction between TIAM1 and CaMKII. (b) Interaction between TIAM1 and CaMKII as visualized by FLIM-FRET before and during structural LTP (top). Warmer hues indicate shorter lifetime and more interaction. The distribution of TIAM1-GFP, as a proxy of structure, is shown (bottom). (Adapted from Saneyoshi et al. (2019) [19])

It is possible that the 720 nm uncaging laser bleeds through into the detector even with a blocking filter. This is readily noticeable in the images as bright horizontal lines at regular intervals. If this occurs, avoid including such images in the analyses.

3. The data from TCSPC are converted to the ASCII format. The analysis of the lifetime images is done with a custom-written macro in Igor Pro (Wavemetrics) [19, 22]. Due to the limited number of photons that can be recorded from a single spine, exponential fitting is difficult. We therefore calculate the average arrival time of all photons, which theoretically equals the decay time of a single exponential decay. We express the results as the difference from the lifetime during the baseline before the glutamate uncaging.

4 Tips

1. If the structural enlargement of the dendritic spine does not last long, it is often because the quality of the slice culture is not optimal. Ensure that the dissection is completed in the shortest time possible. Remove excess medium around the slice during culture. It is also advisable to perform a lot test of the horse serum. A good slice culture will maintain its thickness, while a poor slice culture will flatten during culture.

The flow rate and temperature of the ACSF in the imaging chamber should be stable.

If transfection efficiency is poor, the quality of the gene gun bullets might be compromised. Ensure that there is fresh desiccant in the bullet container. Before opening the container, leave it at room temperature for 20–30 min to prevent the accumulation of moisture.

2. When GFP or another fluorescent protein is used as a volume filler, the fine structure of dendritic spines near the dendritic shaft can be blurred as the shaft is brighter. In such case, use of membrane targeted GFP (such as myristoylated GFP, farnesylated GFP, or GFP with GPI-linker) is helpful. However, the spine volume will not be proportional to the GFP signal intensity.
3. Optimization of the FLIM-FRET sensors needs to be done empirically, such as the location of the fluorescent protein (N-, C-, or middle of the molecule), and the linker between the molecule and the fluorescent proteins.
4. Validation of the biosensor must be performed. For TIAM1-CaMKII, we first identified the interaction interface with alanine scanning and immunoprecipitation from HEK 293 cells

[19]. Then we used an identified mutant as a negative control in FLIM-FRET experiments.

5. Expression of the biosensor itself may cause a phenotype due to overexpression. Although it is difficult to totally avoid such an effect, it is advisable to monitor the density and structure of dendritic spines as well as the efficiency of sLTP in comparison with neurons expressing GFP only.

Acknowledgment

We thank E. Agnello for comments on the manuscript. This work was supported in part by KAKENHI (JP18H05434, JP22H04981, JP22K21353, JP21H05692, JP21H02595, 22H00434, 22H04981, 22K21353) from the Japan Society for the Promotion of Science (JSPS) and the Ministry of Education, Culture, Sports, Science, and Technology (MEXT), ISHIZUE 2022 of Kyoto University (TS), the Takeda Science Foundation (TS, YH), and Human Frontier Science Program RGP0022/2013 and RGP0020/2019, and JST CREST JPMJCR20E4.

References

1. Okamoto K et al (2004) Rapid and persistent modulation of actin dynamics regulates post-synaptic reorganization underlying bidirectional plasticity. *Nat Neurosci* 7(10): 1104–1112
2. Matsuzaki M et al (2004) Structural basis of long-term potentiation in single dendritic spines. *Nature* 429(6993):761–766
3. Nägerl UV et al (2004) Bidirectional activity-dependent morphological plasticity in hippocampal neurons. *Neuron* 44(5):759–767
4. Bosch M, Hayashi Y (2012) Structural plasticity of dendritic spines. *Curr Opin Neurobiol* 22(3):383–388
5. Wiegert JS, Oertner TG (2013) Long-term depression triggers the selective elimination of weakly integrated synapses. *Proc Natl Acad Sci U S A* 110(47):E4510–E4519
6. Saneyoshi T, Hayashi Y (2012) The Ca²⁺ and Rho GTPase signaling pathways underlying activity-dependent actin remodeling at dendritic spines. *Cytoskeleton (Hoboken)* 69(8): 545–554
7. Saneyoshi T (2021) Reciprocal activation within a kinase effector complex: a mechanism for the persistence of molecular memory. *Brain Res Bull* 170:58–64
8. Okamoto K, Bosch M, Hayashi Y (2009) The roles of CaMKII and F-actin in the structural plasticity of dendritic spines: a potential molecular identity of a synaptic tag? *Physiology (Bethesda)* 24:357–366
9. Goto A et al (2021) Stepwise synaptic plasticity events drive the early phase of memory consolidation. *Science* 374(6569):857–863
10. Gu J et al (2010) ADF/cofilin-mediated actin dynamics regulate AMPA receptor trafficking during synaptic plasticity. *Nat Neurosci* 13(10):1208–1215
11. Fukazawa Y et al (2003) Hippocampal LTP is accompanied by enhanced F-actin content within the dendritic spine that is essential for late LTP maintenance in vivo. *Neuron* 38(3): 447–460
12. Herring BE, Nicoll RA (2016) Long-term potentiation: from CaMKII to AMPA receptor trafficking. *Annu Rev Physiol* 78:351–365
13. Matsuzaki M et al (2001) Dendritic spine geometry is critical for AMPA receptor expression in hippocampal CA1 pyramidal neurons. *Nat Neurosci* 4(11):1086–1092
14. Oh WC, Hill TC, Zito K (2013) Synapse-specific and size-dependent mechanisms of spine structural plasticity accompanying synaptic weakening. *Proc Natl Acad Sci U S A* 110(4):E305–E312

15. Takao K et al (2005) Visualization of synaptic Ca²⁺/calmodulin-dependent protein kinase II activity in living neurons. *J Neurosci* 25(12): 3107–3112
16. Ueda Y, Kwok S, Hayashi Y (2013) Application of FRET probes in the analysis of neuronal plasticity. *Front Neural Circuits* 7:163
17. Miyawaki A (2011) Development of probes for cellular functions using fluorescent proteins and fluorescence resonance energy transfer. *Annu Rev Biochem* 80:357–373
18. Yasuda, R., Studying signal transduction in single dendritic spines. *Cold Spring Harb Perspect Biol*, 2012. 4(10).
19. Saneyoshi T et al (2019) Reciprocal activation within a kinase-effector complex underlying persistence of structural LTP. *Neuron* 102(6): 1199–1210.e6
20. Niwa H, Yamamura K, Miyazaki J (1991) Efficient selection for high-expression transfectants with a novel eukaryotic vector. *Gene* 108(2):193–199
21. Stoppini L, Buchs PA, Muller D (1991) A simple method for organotypic cultures of nervous tissue. *J Neurosci Methods* 37(2):173–182
22. Bosch M et al (2014) Structural and molecular remodeling of dendritic spine substructures during long-term potentiation. *Neuron* 82(2):444–459